

A COMBINED EXPERIMENTAL AND THEORETICAL STUDY ON THE FORMATION OF THE AMINO ACID GLYCINE ($\text{NH}_2\text{CH}_2\text{COOH}$) AND ITS ISOMER (CH_3NHCOOH) IN EXTRATERRESTRIAL ICES

PHILIP D. HOLTOM,^{1,2} CHRIS J. BENNETT,³ YOSHIHIRO OSAMURA,⁴ NIGEL J. MASON,² AND RALF I. KAISER^{2,3,5}

Received 2004 December 16; accepted 2005 March 3

ABSTRACT

We have investigated the synthesis of the simplest amino acid, glycine, by Galactic cosmic-ray particles in extraterrestrial ices. Laboratory experiments combined with electronic structure calculations showed that a methylamine molecule [$\text{CH}_3\text{NH}_2(X^1A')$] can be dissociated through interaction with energetic electrons in the track of a cosmic-ray particle to form atomic hydrogen and the radicals $\text{CH}_2\text{NH}_2(X^2A')$ and $\text{CH}_3\text{NH}(X^2A')$. Hydrogen atoms with sufficient kinetic energy could overcome the entrance barrier to add to a carbon dioxide molecule [$\text{CO}_2(X^1\Sigma_g^+)$], yielding a *trans*-hydroxycarbonyl radical, $\text{HOCO}(X^2A')$. Neighboring radicals with the correct geometric orientation then recombine to form glycine, $\text{NH}_2\text{CH}_2\text{COOH}(X^1A)$, and also its isomer, $\text{CH}_3\text{NHCOOH}(X^1A)$. These findings expose for the first time detailed reaction mechanisms of how the simplest amino acid glycine and its isomer can be synthesized via nonequilibrium chemistry in interstellar and cometary ices. Our results offer an important alternative to aqueous and photon-induced formation of amino acids in comets and in molecular clouds. These results also predict the existence of a hitherto undetected isomer of glycine in the interstellar medium, suggest that glycine should be observable on Saturn's moon Titan, and help to account for the synthesis of more complex amino acids in the Murchison and Orgueil meteorites.

Subject headings: astrobiology — astrochemistry — cosmic rays — ISM: general — ISM: molecules — molecular processes

1. INTRODUCTION

The interstellar medium, the vast space between the stars, is a rich reservoir of molecular material ranging from simple diatomic molecules to more complex, astrobiologically important molecules such as cyanopolyacetylenes (Winstanley & Nejad 1996) and the carbon hydrate glycolaldehyde (Butler et al. 2001). During the last several years, observational astronomy has refined its spectroscopic detection methods, and particular attention has been devoted to identifying interstellar biomolecules that may provide important insights into the history of the solar system and the origins of life on Earth (Charnley et al. 2002). Amino acids are classic examples of such molecules, since they are the important building blocks of biological systems in, for instance, proteins. The simplest of these amino acids is glycine, $\text{NH}_2\text{CH}_2\text{COOH}$. Higher homologues of amino acids can be derived from glycine by replacing one hydrogen atom of the methylene group (CH_2) by an organic group (March & Smith 2001).

Numerous searches for interstellar glycine have been conducted since the spectrum of glycine was established in the laboratory more than 30 years ago by Brown et al. (1978). Brown et al. (1979) also conducted the first radio search for glycine in Galactic molecular clouds. While not absolutely confirming the presence of glycine, they tentatively estimated a glycine column density limit of 10^{12} – 10^{14} cm^{-2} in Sgr B2 and

Ori A. Surveys for interstellar glycine, however, are hampered by the intrinsic weakness of the lines being searched for and the problems of contamination of spectra by other molecules (Kuan et al. 2003). A recent survey of three hot molecular cores, Sgr B2(N-LMH), Orion KL, and W51 e1/e2, provided tentative evidence that the neutral form of glycine actually exists in these environments. Kuan et al. (2003) reported 27 glycine lines in 19 different spectral bands with column densities of about 10^{14} cm^{-2} ; this translates to fractional abundances with respect to hydrogen of about 2.1×10^{-10} for Sgr B2, 1.5×10^{-9} for Orion, and 2.1×10^{-10} for W51. Note that amino acids have also been detected in solar system bodies (Cronin et al. 1995). In particular, meteorite samples are a rich source of amino acids: 70 amino acids have been identified in the Murchison meteorite sample alone (Cronin et al. 1995). These amino acids vary in complexity and structure, with both D and L enantiomers being detected.

To date, most laboratory experiments have focused on investigating the liquid synthesis of amino acids and produced 1:1 mixtures of D and L isomers. Biological systems on Earth are almost exclusively based around L-amino acids (Brack 1998). If amino acids are formed in solution, then, at present, there is no explanation for the nonracemic nature of amino acids in terrestrial life (Cohen & Chyba 2000). One of the mechanisms to explain the predominantly levorotatory nature of Earth-based systems arises from the existence of circularly polarized light, which has been detected in OMC-1 in the interstellar medium (Bailey et al. 1998). If amino acids on meteorites are at least partially formed from the effects of ultraviolet (UV) irradiation and not in aqueous parent-body reactions, then an enantiomer excess is possible. Bernstein et al. (2002) and Ehrenfreund et al. (2001) demonstrated that, using unpolarized ultraviolet radiation of an astrophysical ice analog, the amino acids serine and alanine can be produced in a racemic mixture. If the UV light had been circularly polarized, then the formation of excess levorotatory molecules may have been possible. However, to

¹ Department of Physics and Astronomy, University College London, Gower Street, London WC1E 6BT, UK.

² Department of Physics and Astronomy, The Open University, Milton Keynes MK7 6AA, UK.

³ Department of Chemistry, University of Hawaii at Manoa, Honolulu, HI 96822.

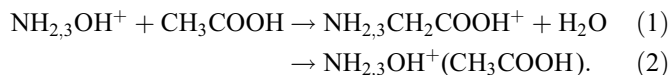
⁴ Department of Chemistry, Rikkyo University, 3-34-1 Nishi-ikebukuro, Tokyo 171-8501, Japan.

⁵ Corresponding author; kaiser@gold.chem.hawaii.edu.

date there have been no experiments performed to test this hypothesis.

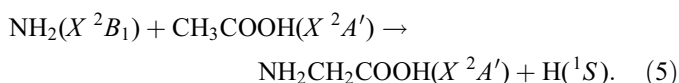
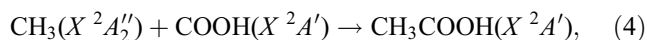
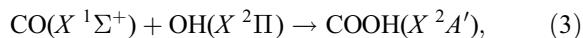
Despite the importance of amino acids in the astrobiological evolution of the interstellar medium and of our solar system, little is known about how these species are actually formed in extraterrestrial environments. Four formation mechanisms have been postulated. These are (1) a formation in the solid state via high-energy particles of the cosmic radiation field, (2) a gas-phase synthesis of amino acids (Blagojevic et al. 2003), (3) in the case of meteoritic material, a synthesis of the amino acids in aqueous solution (Peltzer et al. 1984), and (4) a Urey-Miller-type synthesis. The Urey-Miller experiment was performed for the first time in the 1950s. Miller (1953) showed the formation of amino acids using a simulated primitive Earth environment. By passing an electrical discharge through a simulated primitive Earth environment containing water and an appropriate mixture of the gases methane (CH₄), ammonia (NH₃), water (H₂O), and molecular hydrogen (H₂), it is possible to synthesize amino acids such as glycine, α -alanine, and β -alanine. This approach, however, does not explain the amino acid levorotatory excess on Earth and is limited, as we do not have a complete understanding of the exact conditions of the primitive Earth environment. In addition, modern atmospheric models predict a less strongly reducing environment for the primitive earth, one similar in composition to volcanic outgassing, composed of carbon dioxide (CO₂), nitrogen (N₂) with traces of carbon monoxide (CO), hydrogen (H₂), and reduced sulfur gases (Kasting 1993). Therefore, the validity of these experiments remains questionable.

Blagojevic et al. (2003) investigated gas-phase ion-molecule reactions in the interstellar medium. They were able to produce glycine and β -alanine, as well as acetic and propanoic acid from reactant molecules already detected in the gas phase. Glycine was formed from the reactions of acetic acid with ionized and protonated hydroxylamine via (Blagojevic et al. 2003)



They propose that neutral glycine could then be produced from dissociative recombination and electron-transfer reactions, with dissociative recombination being the favored channel (Blagojevic et al. 2003), since glycine has a high proton affinity.

Sorrell (2001) predicted a possible route to glycine through the UV photoprocessing of water (H₂O), methane (CH₄), ammonia (NH₃), and carbon monoxide (CO) ice mixtures. UV photons from 4 to 13 eV have been postulated to generate radicals such as the hydroxyl (OH), methyl (CH₃), and amino (NH₂) species. Radical-radical reactions may occur with essentially no entrance barrier, so they are speculated to be sources for the formation of complex large organics (Sorrell 2001) via the reaction sequence



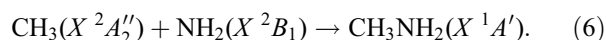
However, in order to react via multiple reaction sequences, these radical species have to diffuse either inside the ices or onto their

surfaces. These diffusive processes involve significant energy barriers (Atkins & de Paula 2001). It therefore is highly unlikely that the reaction sequence (3)–(5) forms the amino acid glycine. In addition, Ehrenfreund et al. (2001) noted that amino acids are susceptible to UV photodestruction. This means that amino acids, once released from the interstellar grain in the hot core phase into the gas phase, are unlikely to exist in large quantities in the interstellar medium.

While gas-phase and solid-state reactions may proceed in the interstellar medium, and complex organic molecules can be formed in photon-screened environments, these organics need a transport mechanism and an environment in which they are protected from the damaging effects of ultraviolet photons. One such favorable site would be on icy dust grains in the interstellar medium or in comets, as any products formed can be protected from the ultraviolet photons deep within the ice layers (Moore et al. 2001). Laboratory studies have shown that substantial chemical reactions can take place on the surfaces of dust grains and comets (Moore et al. 2001). Once they are exposed to (successions of) solar photons, ion irradiation, cosmic rays, and electron bombardment, chemical modifications of the ices can occur and lead to the breakdown and formation of complex chemical species. Munoz Caro et al. (2002) investigated the irradiation of a mixture of water (H₂O), methanol (CH₃OH), ammonia (NH₃), carbon monoxide (CO), and carbon dioxide (CO₂) with a photon flux of $1.5 \times 10^{15} \text{ s}^{-1}$ for 24 hr and found that detectable quantities of amino acids were produced. The residue was analyzed after acid hydrolysis with gas chromatography–mass spectrometry (GC-MS) to detect the levels of amino acids. The authors found glycine to be the most abundant, quoting a quantum yield of $\varphi \approx 3.6 \times 10^{-5}$. This means that one out of 30,000 photons produces a glycine molecule. Note, however, that the authors elucidated neither the basic formation mechanisms (were they actually formed in the ices or during the hydrolysis?) nor the dependence of the quantum yield on the photon wavelength.

Potential reaction pathways to form amino acids have also been investigated theoretically. Woon (2002) utilized quantum chemical modeling of astrophysical ices. He showed that one possible reaction mechanism for the formation of glycine is the recombination of the COOH(X^2A') radical with CH₂NH₂(X^2A'). The most obvious source of the CH₂NH₂ radical seems to be methylamine, CH₃NH₂(X^1A'), which actually has been detected in the interstellar medium toward Sgr B2 and Ori A in its α , $5_{15}-5_{06}$ (73.0 GHz), and s , $4_{14}-4_{04}$ (86.1 GHz), transitions (Kaifu et al. 1974). However, this pathway has not yet been confirmed in laboratory experiments.

The primary aim of this paper is to investigate the formation of the simplest amino acid glycine in well-defined laboratory simulation experiments. Here, binary mixtures of methylamine (CH₃NH₂) and carbon dioxide (CO₂) are prepared at temperatures of 10 K. This temperature is representative for ices condensed on interstellar grain material (Minh & van Dishoeck 2000). The binary ice mixtures simulate the existence of *neighboring* CH₃NH₂–CO₂ complexes on icy grains in dark (molecular) clouds. We would like to stress that so far, methylamine has only been detected in the gas phase of the interstellar medium. However, recent laboratory experiments showed explicitly that methylamine can be formed via recombination of *neighboring* methyl (CH₃; X^2A_2'') and amino radicals (NH₂; X^2B_1) in a matrix cage through (R. I. Kaiser et al. 2005, in preparation)



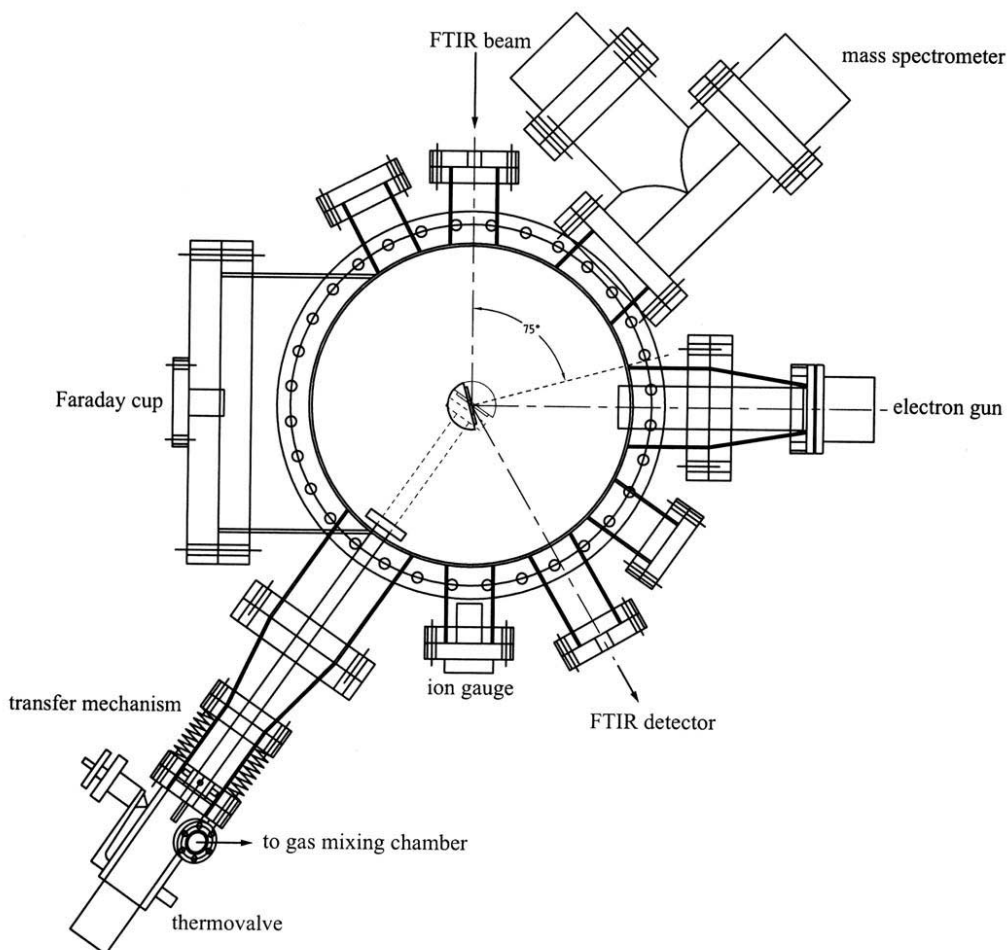


FIG. 1.—Top view of the experimental setup.

Since the methane and ammonia precursor molecules (which can form the methyl and amino radicals via simple C–H and N–H bond rupture processes) have actually been detected on icy grains in molecular clouds (Gürtler et al. 2002), methylamine is expected to exist on interstellar grains as well, but at concentrations of less than 1%—too low to be detected by current infrared spectroscopy observational techniques.

In our experiments the ices are processed by bombardment with 5 keV electrons. We demonstrated earlier that the particles of Galactic cosmic-ray field, which consists of about 98% protons (p , H^+) and 2% helium nuclei (α -particles, He^{+2}) at a distribution maximum of about 10 MeV with $\phi = 10$ particles $cm^{-2} s^{-1}$ (Kaiser & Roessler 1998), lose 99.99% of their kinetic energy via transfer of their kinetic energy to the electronic system of the target molecules (here carbon dioxide and methylamine). This electronic energy transfer generates energetic electrons (δ -electrons) with energies of a few keV perpendicular to the trajectory of the cosmic-ray MeV implant (Bennett et al. 2004). The electronic linear energy transfer of MeV protons to the ice target holds a similar value to the 5 keV electrons used in the present experiments (see § 2). This is not surprising, since Marlowe and TRIM calculations showed that 99% of the energy of the primary MeV cosmic-ray implant is being transferred via electronic interactions to the kinetic energy of energetic electrons with kinetic energies up to a few keV (Kaiser & Roessler 1998). This conclusion gains strong support from previous MeV proton and electron irradiation of cometary-analog

ices (Kobayashi et al. 1995; Kasamatsu et al. 1997). Here the authors found, after a hydrolysis of the irradiated samples, similar production rates of amino acids in MeV proton (which lose 99% of their kinetic energies to the generation of electrons via electronic interaction processes) and electron-irradiated samples. Therefore, our laboratory experiments mimic the formation of glycine in carbon dioxide–methylamine *neighboring* complexes via charged particles through electron energy-loss processes in interstellar ices as condensed on grains in molecular clouds at 10 K. Once the cold cloud passes through the hot molecular core stage, the newly formed glycine molecules can sublime at elevated temperatures to be detected in the gas phase via radio telescopes.

2. EXPERIMENTAL

The simulation experiments were carried out in a contamination-free ultrahigh vacuum (UHV) chamber; the top view of this machine is shown in Figure 1. A detailed description of this vessel is given in Bennett et al. (2004). Briefly, the machine consists of a 15 liter cylindrical stainless steel chamber that can be evacuated down to 8×10^{-11} torr by a magnetically suspended turbopump backed by an oil-free scroll pump. A rotatable, two-stage closed-cycle helium refrigerator is interfaced to the lid of the machine and holds a polished silver monocrystal. This crystal is cooled to 10.8 ± 0.2 K and serves as a substrate for the ice mixture. The ice condensation is assisted by a precision leak valve. The latter is connected to a gas reservoir and is attached on

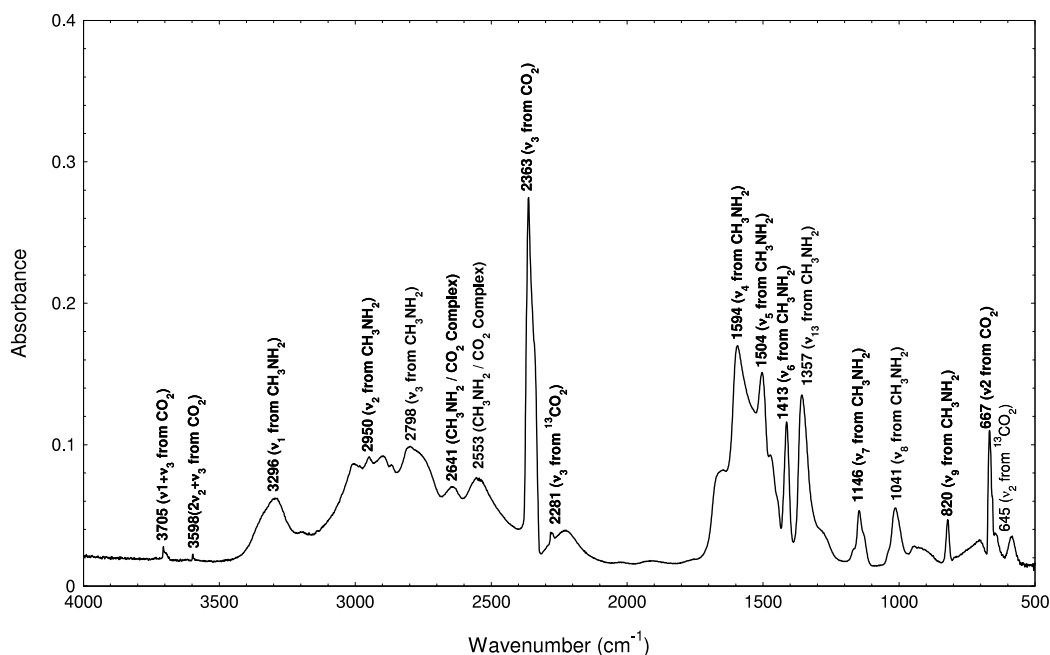


FIG. 2.—Infrared spectrum of the carbon dioxide–methylamine ice at 10 K. The assignments of the peaks are compiled in Table 1.

a linear transfer mechanism. During the gas condensation, the deposition system is moved to be 5 mm in front of the silver target. This experimental setup guarantees a reproducible thickness and composition of the frosts at 10 K. The actual ice sample was prepared at 10 K by depositing binary gas mixtures of methylamine (CH_3NH_2 ; 15 torr, 99.99%) and carbon dioxide (CO_2 ; 10 torr, 99.999%) at a main chamber pressure of 10^{-8} torr for 10 minutes onto the cooled silver crystal. Figure 2 depicts a typical infrared spectrum of the frost at 10 K; the absorptions are compiled in Table 1.

To determine the ice thickness and composition quantitatively, we integrated the infrared absorption features of carbon dioxide at 3708 cm^{-1} (integral absorption coefficient $A = 1.4 \times 10^{-18}\text{ cm}$) and 3600 cm^{-1} ($A = 4.5 \times 10^{-19}\text{ cm}$) and of methylamine at 1600 cm^{-1} ($A = 4.3 \times 10^{-18}\text{ cm}$) and 1150 cm^{-1} ($A = 1.5 \times 10^{-18}\text{ cm}$) and applied a modified Lambert-Beer relationship (Bennett et al. 2004). This suggests a methylamine to carbon dioxide ratio in the ices of about 30. Accounting for the column densities and the densities of carbon dioxide ($1.7 \pm 0.1\text{ g cm}^{-3}$; Klinger et al. 1985) as well as of methylamine ($0.85 \pm 0.05\text{ g cm}^{-3}$; Atoji & Lipscomb 1953), we have an optical thicknesses of $9 \pm 6\text{ nm}$ in carbon dioxide ice and $436 \pm 13\text{ nm}$ in methylamine ice, i.e., a thickness of the binary ice mixture of $445 \pm 19\text{ nm}$. Using the CASINO code (Gauvin et al. 2002), each 5 keV electron loses $2.8 \pm 0.2\text{ keV}$ of its kinetic energy while penetrating the binary ice target; this corresponds to an averaged electronic energy transfer of $5.4 \pm 0.4\text{ keV } \mu\text{m}^{-1}$, i.e., a similar energy loss to that which 10 MeV cosmic-ray protons experience while penetrating the ice [$\text{LET}(10\text{ MeV H}^+) = 4.8 \pm 0.3\text{ keV } \mu\text{m}^{-1}$].

The ices were irradiated at 10 K with 5 keV electrons generated in an electron gun by scanning the electron beam over an area of $3.0 \pm 0.4\text{ cm}^2$. Accounting for the extraction efficiency of 78.8% of the electrons, the target is exposed to 1.8×10^{16} electrons over an irradiation time of 60 minutes. Comparing the electronic linear energy transfer in our experiments to the actual cosmic-ray energy deposition (Kaiser & Roessler 1998), 1 s of our laboratory experiments simulates a processing of interstellar ices over $(1.9 \pm 0.3) \times 10^{11}\text{ s}$. Therefore, our laboratory experiments mimic a

timescale of about 10^7 yr (a typical lifetime of an interstellar cloud).

To guarantee an identification of the reaction products in the ices and those subliming into the gas phase on-line and in situ, a Fourier transform infrared spectrometer (FTIR; solid state) and a quadrupole mass spectrometer (QMS; gas phase) were utilized. The Nicolet 510 DX FTIR spectrometer ($5000\text{--}500\text{ cm}^{-1}$)

TABLE 1
INFRARED ABSORPTIONS OF THE CARBON DIOXIDE–METHYLAMINE MIXTURE
AND ASSIGNMENTS OF THE OBSERVED BANDS AT 10 K

Frequency (cm^{-1})	Molecule	Assignment	Characterization
3705.....	CO_2	$\nu_1 + \nu_3$	Combination
3598.....	CO_2	$2\nu_2 + \nu_3$	Combination
3296.....	CH_3NH_2	ν_1	NH_2 symmetric stretch
3001/2995.....	CH_3NH_2	ν_{11}	CH_3 antisymmetric stretch
2950.....	CH_3NH_2	ν_2	CH_3 antisymmetric stretch
2798.....	CH_3NH_2	ν_3	CH_3 symmetric stretch
2363.....	CO_2	ν_3	Asymmetric stretch
2281.....	$^{13}\text{CO}_2$	ν_3 ($^{13}\text{CO}_2$)	Isotope peak
1594.....	CH_3NH_2	ν_4	NH_2 scissor
1504.....	CH_3NH_2	ν_5	CH_3 antisymmetric deformation
1475.....	CH_3NH_2	ν_{12}	CH_3 antisymmetric deformation
1413.....	CH_3NH_2	ν_6	CH_3 symmetric deformation
1357.....	CH_3NH_2	ν_{13}	NH_2 twist
1167.....	CH_3NH_2	ν_{14}	CH_3 rocking (shoulder)
1146.....	CH_3NH_2	ν_7	CH_3 rocking
1041.....	CH_3NH_2	ν_8	CN stretching (shoulder)
820.....	CH_3NH_2	ν_9	NH_2 wagging
667.....	CO_2	ν_2	In plane/out of plane bending
645.....	CO_2	ν_2 ($^{13}\text{CO}_2$)	Isotope peak

NOTES.—The symmetric stretch fundamental (ν_1) of carbon dioxide at 1384 cm^{-1} is concealed by the ν_{13} fundamental of methylamine at 1357 cm^{-1} . The ν_{15} torsion fundamental of methylamine at 268 cm^{-1} is below our detection range, and the ν_{10} asymmetric stretch fundamental of methylamine at 3427 cm^{-1} is concealed by the ν_1 fundamental of methylamine. Note that the peak at 645 cm^{-1} might be also assigned to a complex formation due to the interaction between the free electron pair from the nitrogen atom and the carbon atom in the carbon dioxide molecule (Dartois et al. 1999).

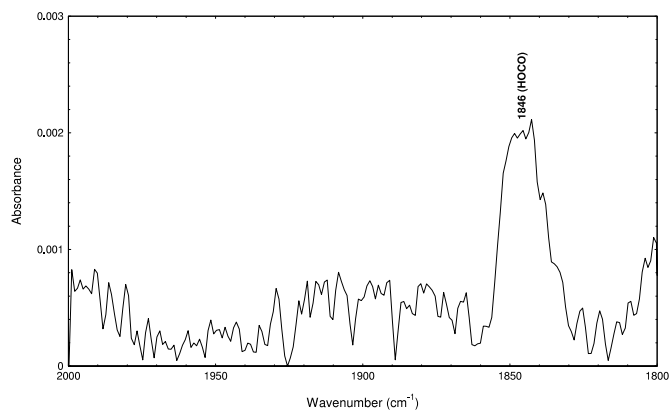


FIG. 3.—HOCO absorption band (1846 cm^{-1}) as seen after a 60 minute irradiation of the sample at 10 K with electrons.

operates in an absorption-reflection-absorption mode (reflection angle $\alpha = 75^\circ$, resolution $0.5\text{--}2\text{ cm}^{-1}$). The infrared beam is coupled via a mirror flipper outside the spectrometer, passes through a differentially pumped potassium bromide (KBr) window, is attenuated in the ice sample prior to and after reflection at a polished silver wafer, and exits the main chamber through a second differentially pumped KBr window before being monitored via a liquid nitrogen-cooled detector. The gas phase is monitored by a quadrupole mass spectrometer (Balzer QMG 420; 1–200 amu mass range) with electron impact ionization of the neutral molecules in the residual gas analyzer mode at electron energies of 100 eV and the photomultiplier operating at 2000 V; the dwell time was chosen to be between 1 s and 0.5 ms. After the irradiation, the sample was kept isothermal at 10 K and warmed up at 0.5 K minute^{-1} to 293 K. The solid residues were then cooled back down to 10 K to record an infrared spectrum.

3. COMPUTATIONAL APPROACH

We have applied the density functional B3LYP methods (Becke 1993; Lee et al. 1988) to optimize the molecular structures of the glycine anion ($\text{NH}_2\text{CH}_2\text{CO}_2^-$) and its $\text{CH}_3\text{NHCO}_2^-$ isomer with the 6-311G(d,p) basis set (Krishnan et al. 1980). Using these structures, we have calculated the vibrational frequencies and infrared intensities, which are compared with the experimental infrared spectra. All computations were carried out using the Gaussian 98 program package (Frisch et al. 2002). The energies stated in the text are corrected with the zero-point vi-

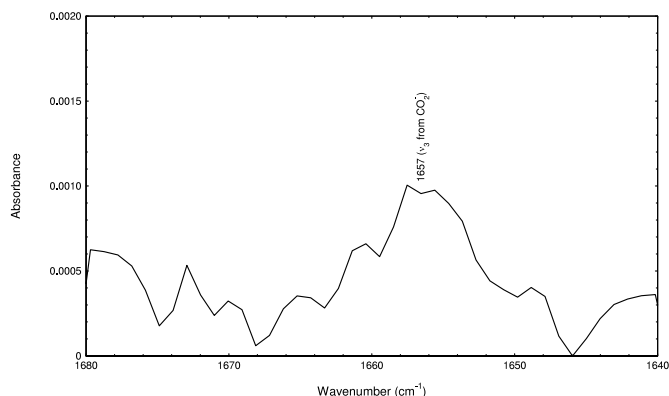


FIG. 4.— CO_2^- absorption band (1657 cm^{-1}) as seen after a 60 minute irradiation of the sample at 10 K with electrons.

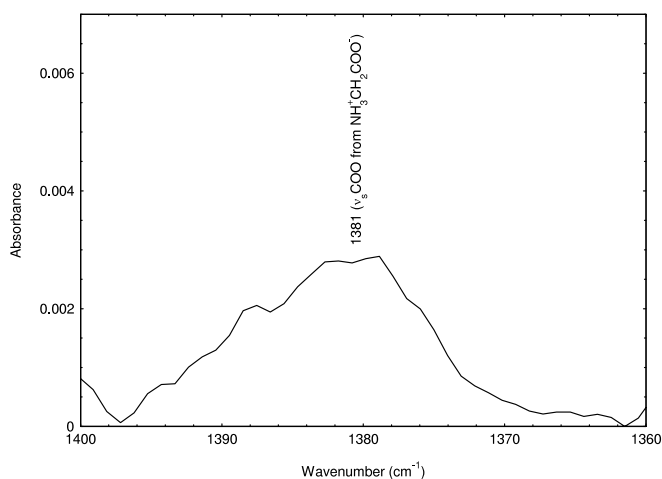


FIG. 5.—Glycine absorption (1381 cm^{-1}) as seen after a 60 minute irradiation of the sample at 10 K with electrons.

brational energies obtained with the B3LYP/6-311G(d,p) level of theory.

4. RESULTS

4.1. Infrared Spectroscopy

The FTIR spectra are analyzed in two steps. First, we investigate the new features qualitatively and assign them to specific transitions. Then we calculate production rates of the synthesized molecules in units of molecules cm^{-2} (column density). The effects of the electron irradiation of the $\text{CH}_3\text{NH}_2/\text{CO}_2$ target at 10 K are shown in Figures 3–5 and are compiled in Table 2. A comparison of the pristine sample (Fig. 2) with the irradiated ice at 10 K shows new absorption features that can be attributed to carbon monoxide [$\text{CO}(X^1\Sigma^+)$] at 2139 cm^{-1} (ν_1 CO stretching). We also observed the ν_2 CO stretching fundamental of $\text{HOCO}(X^2A')$ at 1846 cm^{-1} (Jacox 1988; Fig. 3) and one peak attributed to the CO_2^- ion (X^2A_1) at 1657 cm^{-1} (Fig. 4; Jacox & Thompson 1989). An absorption is also present at 1381 cm^{-1} , which can be attributed to the symmetric COO stretch of zwitterionic glycine (Fig. 5). The position of the peaks is in good agreement with previous measurements of these species (Rosado et al. 1998) listing the ν_s COO feature at 1367 cm^{-1} from theoretical calculations and at 1401 cm^{-1} from an experimental determination.

After electron irradiation, the sample was annealed to 300 K and then recooled to 10 K. Prominent absorption features appear in the region of $1200\text{--}1800\text{ cm}^{-1}$ (Fig. 6; Table 3). Since the peaks overlapped considerably, we have deconvoluted the raw data giving peaks at 1335, 1381, 1416, 1495, 1596, 1667, and 1708 cm^{-1} (Table 3). To assign the carriers unambiguously, we

TABLE 2
NEW INFRARED ABSORPTIONS OF THE PROCESSED SAMPLE AT 10 K AFTER AN IRRADIATION WITH 5 keV ELECTRONS

Frequency (cm^{-1})	Molecule	Assignment	Characterization
1381.....	$\text{NH}_3^+\text{CH}_2\text{COO}^-$	ν_s COO	Symmetric CO_2 stretch
1657.....	CO_2^-	ν_3	OCO asymmetric stretch
1846.....	HOCO	ν_2	CO stretch
2139.....	CO	ν_1	CO stretch

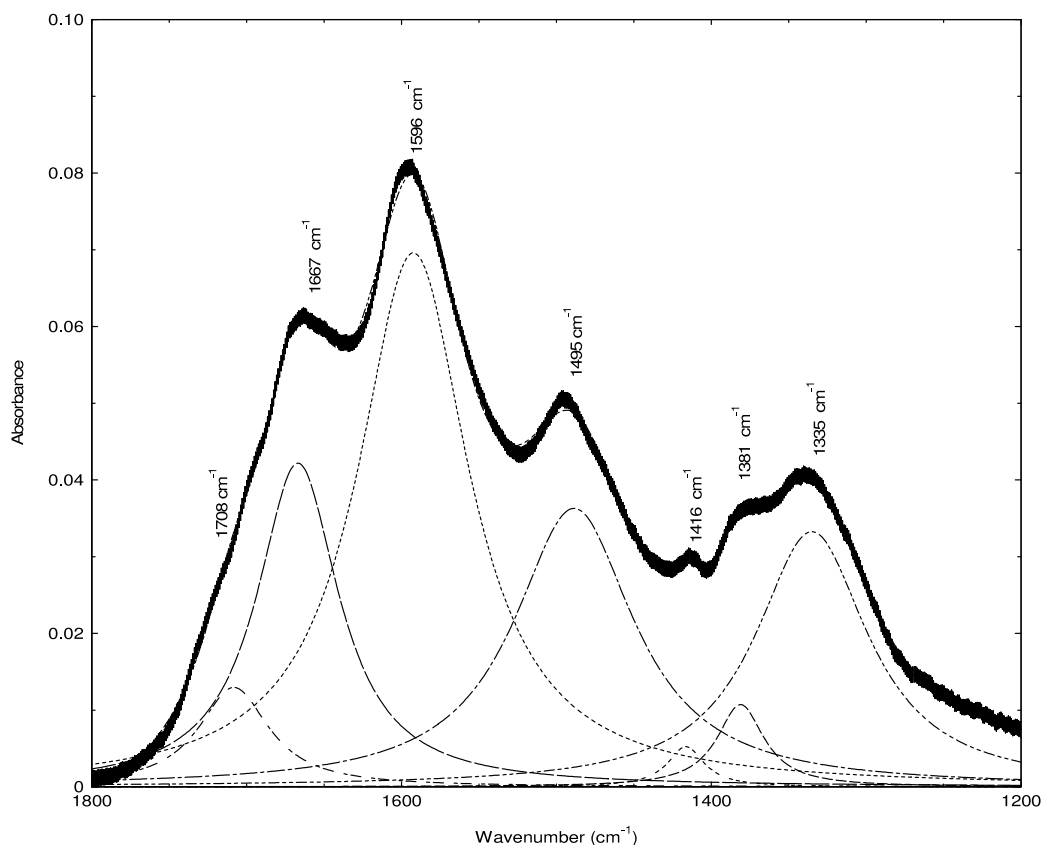


FIG. 6.—Deconvoluted infrared absorptions of the processed sample after warming up to 300 K followed by a successive cooling back to 10 K.

started with the 1381 cm^{-1} band, which was already attributed at 10 K to the $\nu_s(\text{COO})$ fundamental of the glycine zwitterion. To verify this assignment, we identified peaks 1416 ($\nu_s(\text{COO})$), 1495 ($\delta_s(\text{NH}_3)$), and 1596 cm^{-1} ($\nu_{as}(\text{COO})$), which are unique to the glycine zwitterion. Note that on the metal surface, the $\nu_s(\text{COO})$ is actually split up; this correlates nicely with earlier experiments of Rosado et al. (1998). Comparing our data with those of Rosado et al. (1998) yields excellent agreement (Table 4). Here, the bands actually observed hold the largest integrated absorption coefficients in the $1200\text{--}1800\text{ cm}^{-1}$ region (3.86×10^{-17} to $8.77 \times 10^{-17}\text{ cm}$); the remaining absorption coefficients of the glycine zwitterion in this region are less by at least a factor of 3 (Table 4). Integrating the peak areas, accounting for the integral absorption coefficients, we yield a column density of newly synthesized glycine zwitterions of $(2.1 \pm 1.5) \times 10^{16}\text{ cm}^{-2}$. Having assigned the carriers of the zwitterionic glycine, we were able

to allocate the remaining carriers, and we can attribute the 1667 cm^{-1} absorption to the anionic glycine molecule. This value correlated nicely with the calculated one of 1664 cm^{-1} (the anharmonicities have been accounted for by multiplying the unscaled frequencies by a factor of 0.97; this peak actually presents the most intense absorption band of the anionic glycine; Table 5). The 1335 cm^{-1} peak can be assigned either to the ν_9 fundamental of the anionic glycine or to the ω_{CH_2} mode of the zwitterionic glycine. These results suggest column densities of the glycine anion of $(2.8 \pm 1.0) \times 10^{15}\text{ cm}^{-2}$. Finally, the 1708 cm^{-1} feature could be assigned to the ν_5 mode of the isomer of anionic glycine, i.e., $\text{CH}_3\text{NHCO}_2^-$ (Table 6). The position is in very good agreement with the theoretically calculated one of 1699 cm^{-1} ; note that this absorption holds also the highest integrated absorption coefficient of $8.01 \times 10^{-16}\text{ cm}$. Please note that a fraction of the 1381 cm^{-1} absorption, previously assigned to the

TABLE 3
NEW INFRARED ABSORPTIONS OF THE PROCESSED SAMPLE AFTER WARMING UP TO 300 K FOLLOWED BY A SUCCESSIVE COOLING BACK TO 10 K

Frequency (cm^{-1})	Peak Area (cm^{-1})	FWHM (cm^{-1})	$\text{NH}_3^+\text{CH}_2\text{COO}^-$	$\text{NH}_2\text{CH}_2\text{COO}^-$	$\text{CH}_3\text{NHCO}_2^-$
1342.....	3.3	94.3	$\omega\text{ CH}_2$	ν_9	...
1383.....	0.1	21.5	$\nu_s\text{ COO}$...	ν_8
1415.....	0.4	41.4	$\nu_s\text{ COO}$
1493.....	4.3	95.5	$\delta_s\text{ NH}_3$
1595.....	6.2	80.0	$\nu_{as}\text{ COO}$
1662.....	1.7	46.9	...	ν_5	...
1699.....	2.1	68.5	ν_5

TABLE 4
INFRARED ABSORPTION FREQUENCIES OF THE GLYCINE ZWITTERION

Theoretical Wavenumber (cm^{-1})	Integral Absorption Coefficient A (cm molecule^{-1})	Experimental Wavenumber (cm^{-1})	Assignment
3319.....	2.17×10^{-17}	3176, 3040	ν_{as} NH_3
3311.....	1.43×10^{-17}	3176, 3040	ν_{as} NH_3
3224.....	6.46×10^{-18}	2899	ν_s NH_3
2977.....	1.21×10^{-18}	3007	ν_{as} CH_2
2926.....	1.01×10^{-18}	2970	ν_s CH_2
1666.....	8.77×10^{-17}	1596	ν_{as} COO
1616.....	1.81×10^{-17}	1615	δ_{as} NH_3
1614.....	7.36×10^{-18}	1615	δ_{as} NH_3
1493.....	4.39×10^{-17}	1525, 1505	δ_s NH_3
1446.....	1.61×10^{-18}	1460, 1444	δ CH_2
1367.....	3.86×10^{-17}	1413, 1401	ν_s COO
1294.....	1.16×10^{-17}	1334	ω CH_2
1277.....	4.42×10^{-18}	1310	tw CH_2
1046.....	1.43×10^{-18}	1131	NH_3
1025.....	4.7×10^{-18}	1112	ρ NH_3
914.....	1.38×10^{-18}	1034	ν CN
865.....	5.25×10^{-18}	911	ρ CH_2
831.....	1.86×10^{-17}	893	ν CC
648.....	4.98×10^{-19}	698	δ COO
571.....	8.3×10^{-19}	608	ω COO
437.....	3.07×10^{-18}	504	δ CCO
320.....	5.43×10^{-18}	358	δ NCC
206.....	7.97×10^{-19}	520	τ CN
119.....	3.49×10^{-19}	...	τ CC

TABLE 5
CALCULATED HARMONIC INFRARED ABSORPTION FREQUENCIES OF THE MOLECULE $\text{NH}_2\text{CH}_2\text{CO}_2^-$

Assignment	Unscaled Frequency (cm^{-1})	Scaled Frequency (cm^{-1})	Integral Absorption Coefficient A (cm molecule^{-1})
ν_1	3462	3358	2.3×10^{-17}
ν_2	3366	3265	5.8×10^{-17}
ν_3	3038	2947	1.2×10^{-16}
ν_4	2979	2890	1.5×10^{-16}
ν_5	1715	1664	6.9×10^{-16}
ν_6	1681	1630	9.3×10^{-17}
ν_7	1472	1428	3.2×10^{-18}
ν_8	1376	1335	2.8×10^{-17}
ν_9	1360	1319	3.8×10^{-16}
ν_{10}	1288	1249	5.8×10^{-17}
ν_{11}	1153	1118	5.9×10^{-17}
ν_{12}	1121	1087	3.6×10^{-17}
ν_{13}	995	965	2.0×10^{-16}
ν_{14}	942	913	9.8×10^{-18}
ν_{15}	857	831	1.3×10^{-16}
ν_{16}	679	658	2.5×10^{-17}
ν_{17}	573	555	7.8×10^{-18}
ν_{18}	483	468	1.1×10^{-17}
ν_{19}	306	297	3.1×10^{-17}
ν_{20}	238	231	7.1×10^{-17}
ν_{21}	109	106	6.4×10^{-18}

NOTE.—Frequencies were also scaled by a factor of 0.97 to account for the anharmonicity.

TABLE 6
CALCULATED HARMONIC INFRARED ABSORPTION FREQUENCIES OF THE $\text{CH}_3\text{NHCO}_2^-$ MOLECULE

Assignment	Unscaled Frequency (cm^{-1})	Scaled Frequency (cm^{-1})	Integral Absorption Coefficient A (cm molecule^{-1})
ν_1	3555	3448	5.7×10^{-18}
ν_2	3095	3002	1.9×10^{-17}
ν_3	2943	2855	3.0×10^{-16}
ν_4	2857	2771	3.8×10^{-16}
ν_5	1752	1699	8.0×10^{-16}
ν_6	1513	1467	1.8×10^{-17}
ν_7	1489	1444	1.4×10^{-17}
ν_8	1422	1379	1.4×10^{-16}
ν_9	1396	1354	7.2×10^{-17}
ν_{10}	1305	1266	4.4×10^{-16}
ν_{11}	1155	1120	1.3×10^{-16}
ν_{12}	1141	1106	1.7×10^{-17}
ν_{13}	1089	1056	3.1×10^{-17}
ν_{14}	885	858	1.8×10^{-16}
ν_{15}	820	795	7.6×10^{-17}
ν_{16}	739	716	1.0×10^{-16}
ν_{17}	577	560	7.9×10^{-17}
ν_{18}	537	521	2.5×10^{-17}
ν_{19}	300	291	1.6×10^{-17}
ν_{20}	163	158	2.1×10^{-18}
ν_{21}	153	148	4.4×10^{-19}

NOTE.—Frequencies were scaled by a factor of 0.97 to account for the anharmonicity.

glycine zwitterions, could also account for the ν_8 mode of the $\text{CH}_3\text{NHCO}_2^-$ isomer. These data suggest a column density of $(2.7 \pm 1.3) \times 10^{15} \text{ cm}^{-2}$.

4.2. Mass Spectrometry

It is interesting to correlate the infrared observations with the mass spectrometric analysis during the irradiation phase (Fig. 7). During the isothermal state, molecular hydrogen ($m/e = 2$) was observed in the gas phase. We would like to stress that no other molecule was detected to be released into the gas phase during the irradiation process. Therefore, we can exclude that the molecular hydrogen is a fragmentation product of higher molecular products. Note that as we anneal the sample to 13 K, additional hydrogen molecules are released. This finding correlates well with previous studies of silane, d4-silane, and methane ices, which were found to store hydrogen atoms and molecular hy-

drogen even at 10 K to be released during the heating phase (Sillars et al. 2004).

5. DISCUSSION

We must now try to determine the mechanisms by which the glycine zwitterion ($\text{NH}_3^+\text{CH}_2\text{COO}^-$), the anionic glycine ($\text{NH}_2\text{CH}_2\text{COO}^-$), and its $\text{CH}_3\text{NHCOO}^-$ isomer are synthesized in low-temperature methylamine–carbon dioxide ices, both in the irradiation phase at 10 K and/or after heating the target to 300 K. The experimental data can be readily understood in terms of an initial hydrogen loss of the methylamine molecule upon electron irradiation:



Since the methylamine molecule holds two nonequivalent hydrogen atoms at the methyl and the amino group, we can expect the formation of two distinct radicals via a carbon-hydrogen (eq. [7]) and through a nitrogen-hydrogen (eq. [8]) bond rupture process. Our calculations show that both reactions are endoergic by 369 and 394 kJ mol^{-1} , respectively, with the amino-methyl radical, $\text{CH}_2\text{NH}_2(X^2A')$, more stable by 25 kJ mol^{-1} compared to the methyl amino radical, $\text{CH}_3\text{NH}(X^2A')$. Both pathways have also been observed in photodissociation experiments and during collisions of methylamine with metastable noble gases (Tao et al. 1987; Waschewsky et al. 1995; Yang et al. 1997; Hubin-Franskin et al. 2002). Note that this mechanism is similar to the charged particle–induced rupture of the carbon-hydrogen bond in the methane ($\text{CH}_4; X^1A_1$) molecule to form atomic hydrogen and the methyl radical (CH_3) via

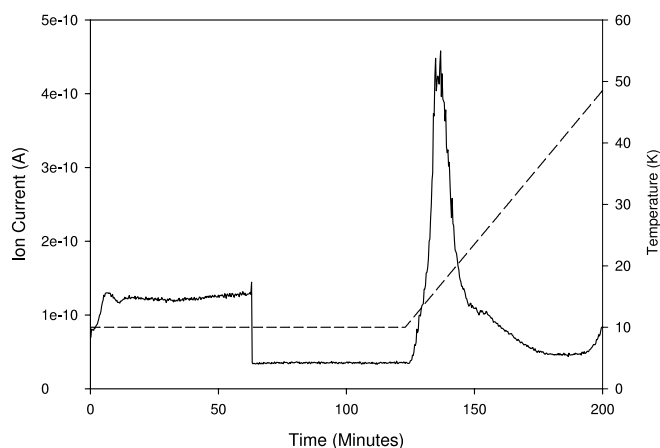
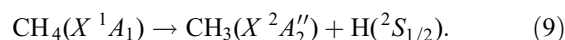


FIG. 7.—Time-evolved mass spectrum showing the evolution of molecular hydrogen in the ice sample together with the temperature of the experiment.

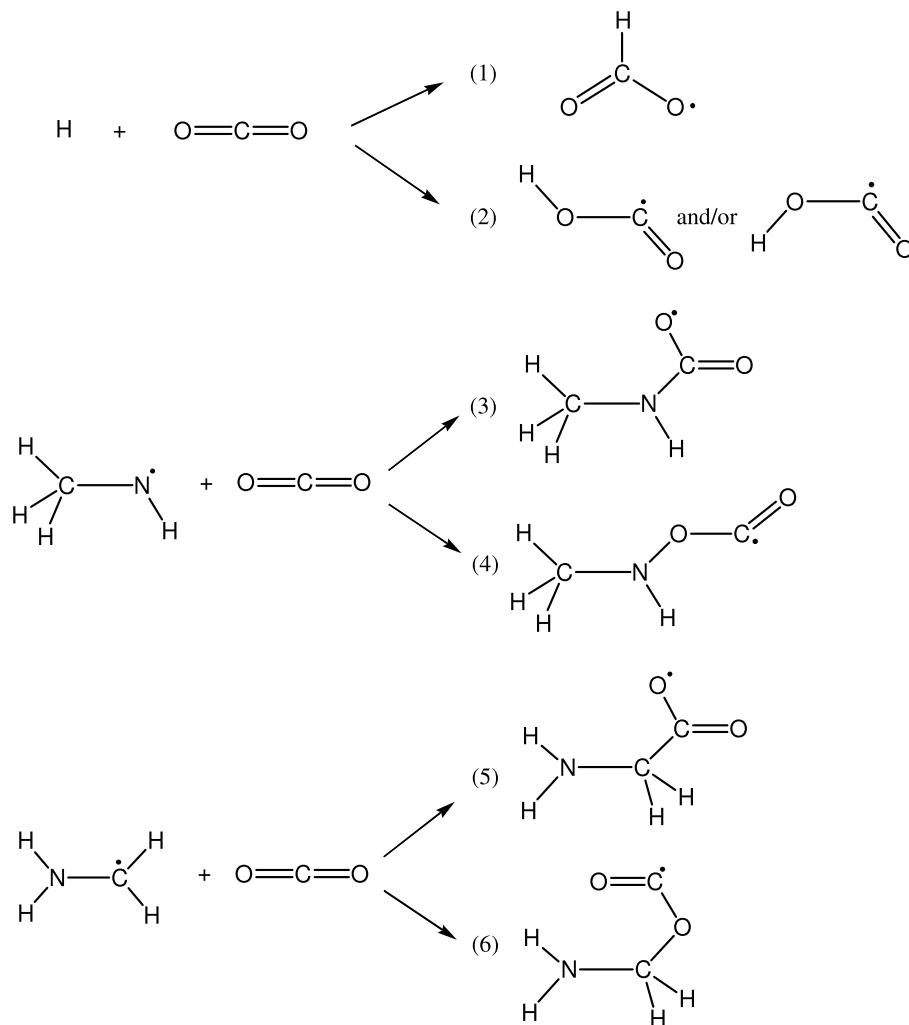
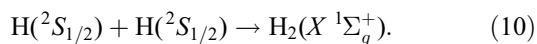


FIG. 8.—Feasible primary reaction pathway in the methylamine–carbon dioxide mixture upon electron irradiation, which may lead to glycine and its isomers. The most stable structure of neutral glycine (in the gas phase) is the confirmation (a) shown in Fig. 9.

However, the intense absorptions of the methylamine matrix do not allow direct infrared spectroscopic detection of the $\text{CH}_2\text{NH}_2(X^2A')$ and $\text{CH}_3\text{NH}(X^2A')$ species. Here, the most intense CH_2 (ν_7 , 615 cm^{-1}) and NH_2 umbrella modes (ν_6 , 697 cm^{-1}), modes of the $\text{CH}_2\text{NH}_2(X^2A')$ radical, and the CH_3 (ν_3 , 2884 cm^{-1} ; ν_2 , 2991 cm^{-1}) asymmetric stretching modes are obscured by the fundamentals of methylamine and carbon dioxide (Table 1; Fig. 2). However, we were able to detect mass spectroscopically molecular hydrogen at $m/e = 2$, i.e., a recombination product of two hydrogen atoms inside the ice sample (Kaiser & Roessler 1998):

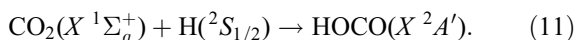


What is the fate of the generated the $\text{CH}_2\text{NH}_2(X^2A')$, $\text{CH}_3\text{NH}(X^2A')$, and $\text{H}(^2S_{1/2})$ species? These open-shell reactants can interact via multiple reaction pathways with a matrix isolated carbon dioxide molecule, as shown in Figure 8. First, the hydrogen atom can interact with the π bond of the carbon dioxide molecule and can add either to the carbon atom (pathway [1] of Fig. 8) or to the oxygen atom (pathway [2] of Fig. 8). The corresponding reaction energies are $+65.6$ and -3.3 kJ mol^{-1} (Zhu et al. 2001). Alternatively, the $\text{CH}_3\text{NH}(X^2A')$ and $\text{CH}_2\text{NH}_2(X^2A')$ radicals can follow a similar reaction scheme

via reactions (3)–(6) in Figure 8. Note that these processes are endoergic by 27, 227, 108, and 95 kJ mol^{-1} .

What is the dominant reaction pathway? We can compare the schematic reaction sequence (Fig. 8) with the experimentally observed species after the irradiation at 10 K (Table 2). Here, we identified the *trans*- $\text{HOCO}(X^2A')$ radical via the $\text{C}=\text{O}$ stretching mode at 1846 cm^{-1} . This suggests that at least route (2) is open at 10 K. Although the pristine sample does not absorb between 1700 and 2000 cm^{-1} , we were unable to observe any of the most intense bands of the $\text{CH}_3\text{NHOCO}(X^2A')$ radical at 1813 , 1841 , and 1860 cm^{-1} (pathway [4] of Fig. 8) or of the $\text{NH}_2\text{CH}_2\text{OCO}(X^2A')$ radical at 1774 , 1762 , and 1813 cm^{-1} (pathway [6] of Fig. 8). The strongest absorptions of $\text{CH}_3\text{NHCOO}(X^2A')$ and $\text{NH}_2\text{CH}_2\text{COO}(X^2A')$ at 1612 and 632 cm^{-1} are obscured by the pure ices in the sample. Therefore, the *trans*-hydroxycarbonyl radical, $\text{HOCO}(X^2A')$, is the only species of the reaction pathways (1)–(6) in Figure 8 that has been positively identified so far. This scenario can be readily understood in terms of the dynamics of the reactions. Assume, for example, that 200 kJ mol^{-1} is available after the initial rupture of the hydrogen-nitrogen bond. In a simple gas-phase model, angular momentum conservation dictates that the majority of the available energy is channeled into kinetic energy of the light particle (here $193.47\text{ kJ mol}^{-1}$ for the hydrogen atom), whereas only a small fraction goes into kinetic energy of

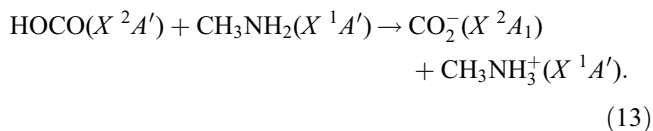
the heavy particle [here 6.6 kJ mol^{-1} for the $\text{CH}_3\text{NH}(X^2A')$ and $\text{CH}_2\text{NH}_2(X^2A')$ radicals]. Note that for the polyatomic radicals, this presents an upper limit due to the rotational and vibrational excitation of the radical species. In the solid state, the hydrogen atom is not in thermal equilibrium with the 10 K matrix and therefore must be defined as suprathreshold. The excess kinetic energy of the hydrogen atom can then be utilized to overcome the entrance barrier of addition of 113 kJ mol^{-1} of the reaction to form the $\text{HOCO}(X^2A')$ radical (Morton & Kaiser 2003; Yu et al. 2001; Zhu et al. 2001); the latter can then be stabilized in the surrounding matrix via phonon coupling. Similarly, vibrational energy in the polyatomic species can be used to compensate for the endoergicity and the involved entrance barriers of pathways (3)–(8) in Figure 8, as well. However, vibrationally excited polyatomic species are more likely to couple their internal energy to the surrounding matrix via phonon interaction. This effect has been observed in the CH_4/CO system (Bennett et al. 2005), where the methane molecule was cleaved upon electron irradiation via equation (9), and only the hydrogen atom was found to react with the carbon monoxide molecule to form the spectroscopically observed formyl radical ($\text{HCO}; X^2A'$); no product of the methyl radical plus carbon monoxide reaction could be observed. We therefore suggest that upon release of a hydrogen atom from the methylamine molecule via equations (7) and/or (8), the suprathreshold hydrogen atom overcomes the barrier to addition forming the spectroscopically observed *trans*-hydroxyl radical, $\text{HOCO}(X^2A')$, in an exoergic reaction ($-14.6 \text{ kJ mol}^{-1}$) via



Since the reaction is exoergic, and hence the transition state is “early,” kinetic energy is very efficient to overcome the entrance barrier (Steinfeld et al. 1998). It is important to stress that we observed not only the $\text{HOCO}(X^2A')$ radical, but also the $\text{CO}_2^-(X^2A_1)$ anion at 1657 cm^{-1} . Two pathways are likely to form this anion, i.e., a reduction of the carbon dioxide molecule, which is correlated with an acceptance of the electron in the lowest unoccupied molecular orbital of the carbon dioxide molecule (scenario 1),

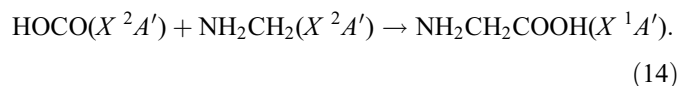


or a proton transfer from the *trans*-hydroxylcarbonyl species (an acid) to a methylamine molecule in the matrix (a base; scenario 2),



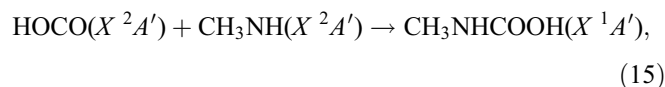
Since we did not observe any $\text{CO}_2^-(X^2A_1)$ anion during the irradiation of a pure carbon dioxide ice at identical temperatures, irradiation currents, and electron energies (Bennett et al. 2004), we suggest that a proton transfer process is more likely. Note that we also detect the strongest fundamental of the $\text{CH}_3\text{NH}_3^+(X^2A')$ cation at 3355 cm^{-1} (ν_7). To form the amino acid glycine, the $\text{HOCO}(X^2A')$ species has to react with the $\text{CH}_2\text{NH}_2(X^2A')$ radical. However, since the latter is immobile at 10 K, the reaction must take place between neighboring

radicals that hold the correct reaction geometry in the matrix cage via



Recall that this radical-radical recombination reaction requires no entrance barrier and hence is feasible at 10 K. However, we were not able to detect any absorption of the neutral glycine conformers, although the 1810, 1778, 1784, and 1808 cm^{-1} absorptions are not obscured by any absorption from the matrix material (Reva et al. 1995; Ivanov et al. 1998; Alexandrov et al. 1998). Instead, we identified the zwitterionic form of the glycine molecule at 1381 cm^{-1} (Table 2) at column densities of $(1.2 \pm 0.2) \times 10^{13} \text{ cm}^{-2}$. Therefore, the data suggest that in the alkaline methylamine matrix, the glycine molecule may undergo a proton transfer to the zwitterionic structure at 10 K. We would like to stress that the overall reaction to form neutral glycine from the methylamine and carbon dioxide reactants has been calculated to be endoergic by, depending on the glycine conformer, at least 41 kJ mol^{-1} (Fig. 9). This also underlines the necessity of non-equilibrium (suprathreshold) chemistry to actually synthesize glycine via energetic particle and nonthermal sample processing.

The arguments developed in the previous paragraphs help us to understand the spectroscopic detection and the formation mechanism of the glycine zwitterion in the low-temperature matrix. We attempt now to rationalize the enhanced column density of the glycine zwitterion [$\text{NH}_3^+\text{CH}_2\text{COO}^-$, $(2.1 \pm 1.5) \times 10^{16} \text{ cm}^{-2}$] and the observation of anionic glycine [$\text{NH}_2\text{CH}_2\text{COO}^-$, $(2.8 \pm 1.0) \times 10^{15} \text{ cm}^{-2}$] and its $\text{NH}_2\text{CH}_2\text{COO}^-$ isomer [$(2.7 \pm 1.3) \times 10^{15} \text{ cm}^{-2}$] after warming the sample to 300 K followed by a successive recooling to 10 K. The enhancement of the column density by 3 orders of magnitude after the heating process of the glycine zwitterion suggests an additional, temperature-dependent production route upon warming the ice sample. Here, the annealing phase and hence the enhanced temperature may increase the mobility and hence diffusion coefficient of matrix isolated $\text{HOCO}(X^2A')$, $\text{CH}_3\text{NH}(X^2A')$, and $\text{CH}_2\text{NH}_2(X^2A')$ radicals. Since a radical-radical recombination involves no entrance barrier, a reaction of the *trans*-hydroxylcarbonyl radical with $\text{CH}_3\text{NH}(X^2A')$ and $\text{CH}_2\text{NH}_2(X^2A')$ could explain the formation of additional carbon-carbon and carbon-nitrogen single bonds. However, we were not able to observe any glycine molecules or its isomers, but only the glycine zwitterion as well as the $\text{NH}_2\text{CH}_2\text{COO}^-$ and $\text{CH}_3\text{NHCOO}^-$ anions. This is likely to be an effect of the silver substrate on which these species are adsorbed. Barlow et al. (1998) suggested that upon chemisorption of neutral glycine on metal surfaces such as copper {110}, a fraction of the glycine molecules can donate a proton, and the resulting ion forms a complex and/or chemical bond with the metal surface. The identification of the $\text{CH}_3\text{NHCOO}^-$ anion also presents a further proof that upon annealing of the matrix, the hydroxycarbonyl radical can also recombine with the thermodynamically less stable methyl amino radical, $\text{CH}_3\text{NH}(X^2A')$,



followed by a chemisorption of the corresponding anion to the metal surface; the latter has been formed via equation (8).

Finally, we would like to investigate whether the experimentally observed column densities [$\text{NH}_3^+\text{CH}_2\text{COO}^-$, $(2.1 \pm 1.5) \times 10^{16} \text{ cm}^{-2}$; $\text{NH}_2\text{CH}_2\text{COO}^-$, $(2.8 \pm 1.0) \times 10^{15} \text{ cm}^{-2}$;

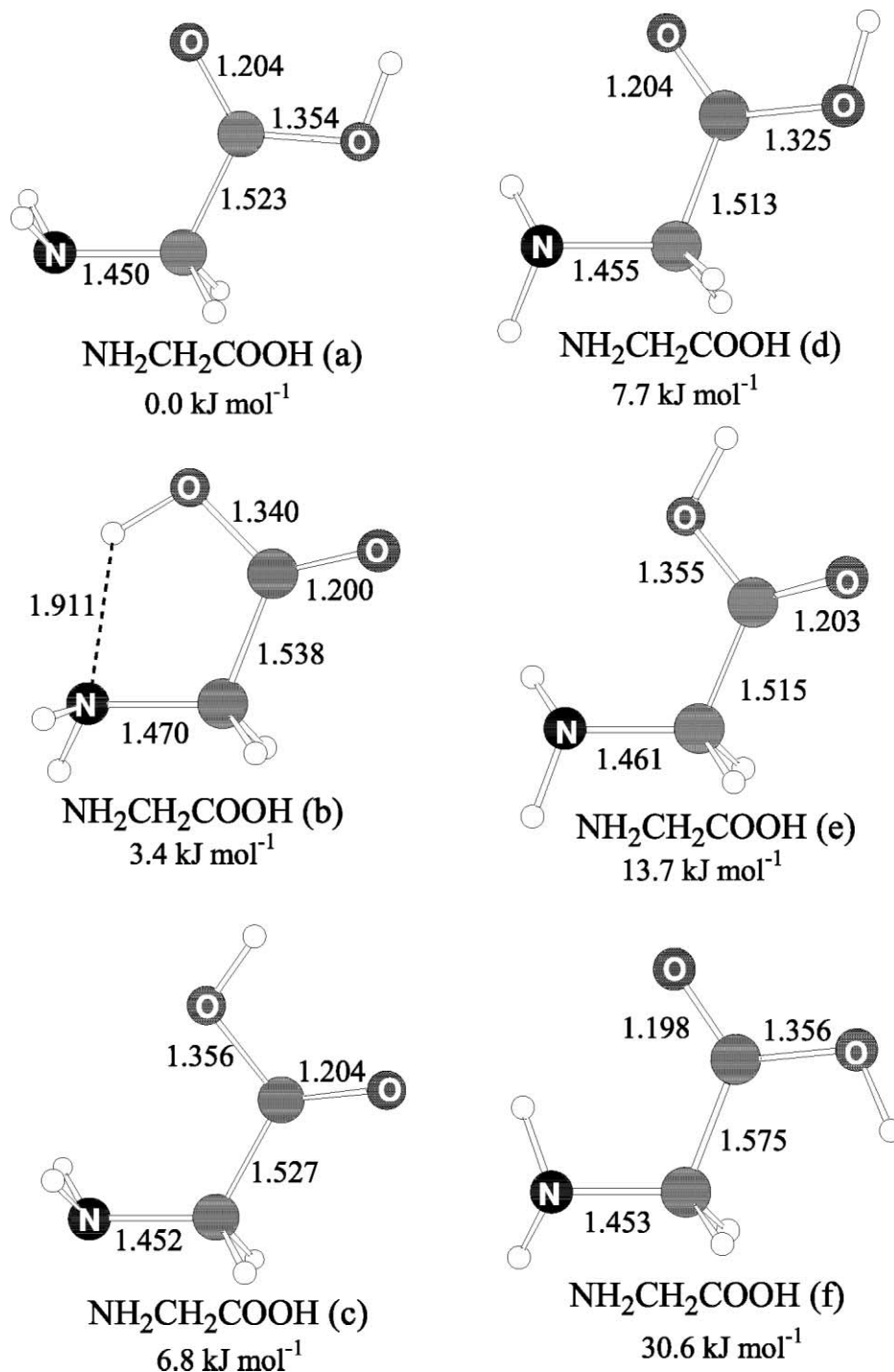


FIG. 9.—Optimized structures of glycine, $\text{NH}_2\text{CH}_2\text{COOH}$, obtained with the B3LYP/6-311G(d,p) level of theory. Relative energies are shown in kJ mol^{-1} corrected with zero-point vibrational energies. Bond lengths are shown in angstroms.

$\text{CH}_3\text{NHCOO}^-$, $(2.7 \pm 1.3) \times 10^{15} \text{ cm}^{-2}$] can be supported energetically. Here, $(2.4 \pm 1.5) \times 10^{16} \text{ cm}^{-2} \text{ CH}_2\text{NH}_2(X^2A')$ and $(2.8 \pm 1.0) \times 10^{15} \text{ cm}^{-2} \text{ CH}_3\text{NH}(X^2A')$ have to be generated. Accounting for the bond dissociation energies and the target surface, $(3.0 \pm 0.5) \times 10^{17} \text{ eV}$ are necessary to cleave the carbon-hydrogen and nitrogen-hydrogen bonds; in addition, each hydrogen atom must have an excess energy of at least 1.1 eV to overcome the barrier of addition to the carbon dioxide molecule. This accounts for an additional $(0.80 \pm 0.1) \times 10^{17} \text{ eV}$, i.e., summing up to $(3.8 \pm 0.4) \times 10^{17} \text{ eV}$. Considering the total energy deposition of the implanted electrons of $(5.1 \pm 0.5) \times$

10^{19} eV into the target, the experimentally observed column densities can be synthesized here, but only about $0.7\% \pm 0.2\%$ of the available energy is utilized to form the glycine zwitterion and its anion together with its isomer.

6. ASTROPHYSICAL IMPLICATIONS

Our experiments are the very first step to a systematic understanding of the formation of amino acids (glycine being the simplest member) in extraterrestrial ices found in cold molecular clouds, comets, and in our outer solar system. The explicit identification of the amino acid glycine at low temperature (10 K)

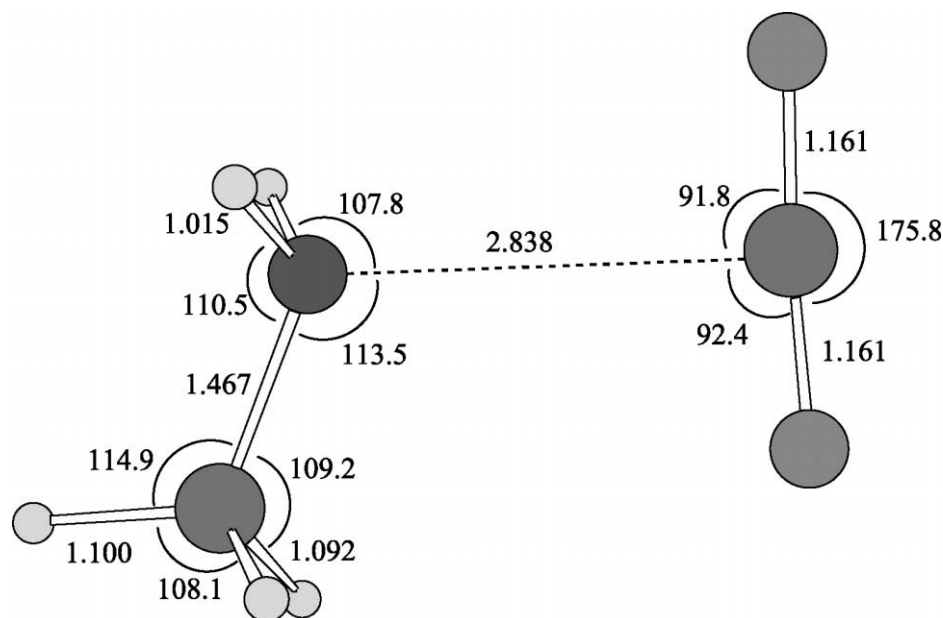
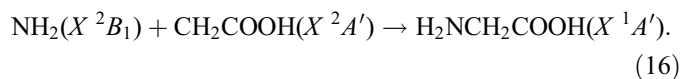


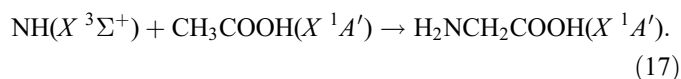
FIG. 10.—Optimized structure of the van der Waals complex between methylamine and carbon dioxide obtained with the B3LYP/6-311G(d,p) level of calculation. The bond length and bond angles are in angstroms and degrees, respectively. The binding energy is calculated to be 12.9 kJ mol⁻¹.

suggests that energetic δ -electrons, which are generated in the ultra track of Galactic cosmic-ray particles penetrating ice samples, primarily induce a carbon-hydrogen bond rupture process in the methylamine molecule $\text{CH}_3\text{NH}_2(X^1A')$ to generate a $\text{CH}_2\text{NH}_2(X^2A')$ radical plus atomic hydrogen. Based on energy and angular momentum conservation, most of the excess kinetic energy is given in the form of translational (kinetic) energy to the light hydrogen atom. The $\text{CH}_2\text{NH}_2(X^2A')$ radical also gets vibrationally excited but, because of its larger mass, is unable to diffuse inside the ice matrix. The vibrational excitation can be coupled into the phonon modes of the ice sample. The generated hydrogen atom is not in thermal equilibrium with its surrounding 10 K (hence, suprathreshold hydrogen atom) and can add to the carbon dioxide molecule to form the *trans*-hydroxycarbonyl, $\text{HOCO}(X^2A')$, radical. If both the $\text{CH}_2\text{NH}_2(X^2A')$ and the $\text{HOCO}(X^2A')$ radicals are formed in the same matrix cage and if they are in a proper geometric orientation with respect to both radical centers, then they can recombine to form the amino acid glycine. The overall reaction was found to be endoergic by at least 41 kJ mol⁻¹, thus underlining the crucial involvement of suprathreshold reactants; the formation of the latter can be triggered by Galactic cosmic-ray particles and the inherent formation of δ -electrons. We would like to stress that we also investigated the energetics of forming glycine in a bound methylamine–carbon dioxide van der Waals cluster (Fig. 10). Here, the endoergicity is actually increased by about 13 kJ mol⁻¹. It is important to outline that the production rates of glycine at 10 K during the irradiation process are very small (smaller by a factor of 500) compared to the glycine column density found after the warming up period to 293 K and recooling of the residue back to 10 K. Note that the 10 K matrix stores a significant amount of HOCO and $\text{CH}_2\text{NH}_2/\text{CH}_3\text{NH}$ radicals, which are immobile at 10 K. The warming up period, simulating the transition from a cold molecular cloud to the hot core stage, also triggers a diffusion and hence possible recombination of the radical species that are not mobile at 10 K. Therefore, nonequilibrium chemistry, which initially generates

the radical species, *and* the thermal processing of the irradiated grain particles are both important components of the synthesis of glycine on interstellar grain particles. Once the glycine has been formed on interstellar grains in, for example, photon-shielded molecular clouds such as Barnard 68 (B68), these species can sublime once the cloud reaches the hot molecular core stage. However, the nascent gas-phase abundances can be altered and hence reduced dramatically, since amino acids were found to be very susceptible to photon destruction, in particular if the hot star heats the grain particles (Ehrenfreund et al. 2001). We would like to stress that at the present stage, we cannot rule out the involvement of the CO_2^- anion in our experimental conditions or the recombination with $\text{CH}_2\text{NH}_2(X^2A')$ and/or $\text{CH}_3\text{NH}(X^2A')$ to form $\text{NH}_2\text{CH}_2\text{COO}^-$ and $\text{CH}_3\text{NHCOO}^-$, respectively. This is currently under investigation. In addition, it should be pointed out that alternative production routes may exist in low-temperature ices, which involve nonequilibrium chemistry. These are, for instance, radical-radical recombination of an amino radical ($\text{NH}_2; X^2B_1$), generated via a cosmic-ray particle-induced nitrogen-hydrogen bond cleavage in an ammonia molecule, with the $\text{CH}_2\text{COOH}(X^2A')$ radical, formed by a carbon-hydrogen bond cleavage of the neutral acetic acid molecule,



Alternatively, suprathreshold NH radicals, which can be formed via Coulomb explosions in the infra track of cosmic-ray particles, can insert into the carbon-hydrogen bond of the acetic acid molecule to form glycine in a one-step, formally spin-forbidden reaction sequence,



These processes are also currently under investigation. The elucidation of formation mechanisms of more complex amino acids is currently underway. We would like to stress again that the laboratory experiments mimic the existence of methylamine-carbon dioxide complexes inside interstellar ices. Therefore, a quantitative extrapolation of our results to interstellar ices is not an easy task; future experiments will investigate the effect of water-dominated ices with small amounts of carbon dioxide-methylamine admixtures. Nevertheless, this will not influence the conclusions drawn about the generalized reaction mechanism to form glycine and its isomers, but it will have implications on the absolute production rates of both isomers.

This work was supported by the Particle Physics and Astronomy Research Council (PPARC, UK; P. D. H., N. J. M., and R. I. K.), the Engineering and Physical Sciences Research Council (EPSRC, UK; P. D. H.), the University of Hawaii at Manoa (C. J. B. and R. I. K.), and the NASA-Astrobiology Institute (C. J. B. and R. I. K.). We are also grateful to Ed Kawamura and Dave Kempton (University of Hawaii, Department of Chemistry) for their electrical and mechanical work. The computations were carried out at the computer center of the Institute for Molecular Science, Japan, and partly supported by the Grants-in-Aid for Scientific Research on Priority Areas from the Ministry of Education, Science, and Culture, Japan (Y. O.).

REFERENCES

- Alexandrov, V., Stepanian, S., & Adamowicz, L. 1998, *Chem. Phys. Lett.*, 291, 110
- Atkins, P. W., & de Paula, J. 2001, *Physical Chemistry* (7th ed.; Oxford: Oxford Univ. Press)
- Atoji, M., & Lipscomb, W. N. 1953, *Acta Crystallogr.*, 6, 770
- Bailey, J. M., Chrysostomous, A., Hough, J. H., Gledhill, T. M., McCall, A., Clark, S., Ménard, F., & Motohide, T. 1998, *Science*, 281, 672
- Barlow, S. M., Kitching, K. J., Haq, S., & Richardson, N. V. 1998, *Surface Sci.*, 401, 322
- Becke, A. D. 1993, *J. Chem. Phys.*, 98, 5648
- Bennett, C. J., Jamieson, C., Kaiser, R. I., & Osamura, Y. 2005, *ApJ*, in press
- Bennett, C. J., Jamieson, C., Mebel, A., & Kaiser, R. I. 2004, *Phys. Chem. Chem. Phys.*, 6, 735
- Bernstein, M. P., Dworkin, J. P., Sandford, S. A., Cooper, G. W., & Allamandola, L. J. 2002, *Nature*, 416, 401
- Blagojevic, V., Petrie, S., & Bohme, D. K. 2003, *MNRAS*, 339, L7
- Brack, A., ed. 1998, *The Molecular Origins Of Life: Assembling the Pieces of the Puzzle* (Cambridge: Cambridge Univ. Press)
- Brown, R. D., Godfrey, P. D., Storey, J. W. V., & Bassez, M. P. 1978, *J. Chem. Soc. Chem. Commun.*, 547
- Brown, R. D., et al. 1979, *MNRAS*, 186, 5P
- Butler, R. A. H., De Lucia, F. C., Petkie, D. T., Møllendal, H., Horn, A., & Herbst, E. 2001, *ApJS*, 134, 319
- Charnley, S. B., Rodgers, S. D., Kuan, Y. J., & Huang, H. C. 2002, *Adv. Space Res.*, 30, 1419
- Cohen, B. A., & Chyba, C. F. 2000, *Icarus*, 145, 272
- Cronin, J. R., Cooper, G. W., & Pizzarello, S. 1995, *Adv. Space Res.*, 15(3), 91
- Dartois, E., Demyk, K., d'Hendecourt, L., & Ehrenfreund, P. 1999, *A&A*, 351, 1066
- Ehrenfreund, P., Bernstein, M. P., Dworkin, J. P., Sandford, S. A., & Allamandola, L. J. 2001, *ApJ*, 550, L95
- Frisch, M. J., et al. 2002, *Gaussian 98* (rev. A11; Pittsburgh: Gaussian, Inc.)
- Gauvin, R., Drouin, D., & Couture, A. R. 2002, *CASINO: Monte Carlo Simulation of Electron Trajectory in Solids* (ver. 2.42; Sherbrooke: Univ. Sherbrooke)
- Gürtler, J., Klaas, U., Henning, T., Abraham, P., Lemke, D., Schreyer, K., & Lehmann, K. 2002, *A&A*, 390, 1075
- Hubin-Franskin, M.-J., et al. 2002, *J. Chem. Phys.*, 116, 9261
- Ivanov, A. Y., Sheina, G., & Blagoi, Y. P. 1998, *Spectrochim. Acta A*, 55, 219
- Jacox, M. E. 1988, *J. Chem. Phys.*, 88, 4598
- Jacox, M. E., & Thompson, W. E. 1989, *J. Chem. Phys.*, 91, 1410
- Kaifu, N., Morimoto, M., Nagane, K., Akabane, K., Iguchi, T., & Takagi, K. 1974, *ApJ*, 191, L135
- Kaiser, R. I., & Roessler, K. 1998, *ApJ*, 503, 959
- Kasamatsu, K., et al. 1997, *Bull. Chem. Soc. Japan*, 70, 1021
- Kasting, J. F. 1993, *Science*, 259, 920
- Klinger, J., Benest, D., Dollfus, A., & Smoluchowski, R., eds. 1985, *Proc. Adv. Res. Workshop, Ices in the Solar System* (Dordrecht: Reidel)
- Kobayashi, K., Kasamatsu, T., Kaneko, T., Koike, J., Oshima, T., Saito, T., Yamamoto, T., & Yanagawa, H. 1995, *Adv. Space Res.*, 16(2), 21
- Krishnan, R., Binkley, J. S., Seeger, R., & Pople, J. A. 1980, *J. Chem. Phys.*, 72, 650
- Kuan, Y., Charnley, S. B., Huang, H., Tseng, W., & Kisiel, Z. 2003, *ApJ*, 593, 848
- Lee, C., Yang, W., & Parr, R. G. 1988, *Phys. Rev. B*, 37, 785
- March, J., & Smith, M. 2001, *March's Advanced Organic Chemistry: Reactions, Mechanisms and Structure* (5th ed.; New York: Wiley)
- Miller, S. L. 1953, *Science*, 117, 528
- Minh, Y. C., & van Dishoeck, E. F., eds. 2000, *IAU Symp. 197, Astrochemistry: From Molecular Clouds to Planetary Systems* (San Francisco: ASP)
- Moore, M. H., Hudson, R. L., & Gerakines, P. A. 2001, *Spectrochim. Acta A*, 57, 843
- Morton, R. J., & Kaiser, R. I. 2003, *Planet. Space Sci.*, 51, 365
- Munoz Caro, G. M., et al. 2002, *Nature*, 416, 403
- Peltzer, E. T., Bada, J. L., Schlesinger, G., & Miller, S. L. 1984, *Adv. Space Res.*, 4(12), 69
- Reva, I. D., Plokhhotnichenko, A. M., Stepanian, S. G., Ivanov, A. Y., Radchenko, E. D., Sheina, G. G., & Blagoi, Y. P. 1995, *Chem. Phys. Lett.*, 232, 141
- Rosado, M. T., Duarte, M. L. T. S., & Fausto, R. 1998, *Vibrational Spectrosc.*, 16, 35
- Sillars, D., Bennett, C. J., Osamura, Y., & Kaiser, R. I. 2004, *Chem. Phys. Lett.*, 932, 541
- Sorrell, W. H. 2001, *ApJ*, 555, L129
- Steinfeld, J. I., Francisco, J. S., & Hase, W. L. 1998, *Chemical Kinetics and Dynamics* (2nd ed.; Paramus: Prentice Hall)
- Tao, W., Golde, M. F., Ho, G. H., & Moyle, A. M. 1987, *J. Chem. Phys.*, 87, 1045
- Waschewsky, G. C. G., Kitchen, D. C., Browning, P. W., & Butler, L. J. 1995, *J. Phys. Chem.*, 99, 2635
- Winstanley, N., & Nejad, L. A. M. 1996, *Ap&SS*, 240, 13
- Woon, D. E. 2002, *ApJ*, 571, L177
- Yang, X., Lin, J., Lee, Y. T., Blank, D. A., Suits, A. G., & Wodtke, A. M. 1997, *Rev. Sci. Instrum.*, 68, 3317
- Yu, H.-G., Muckerman, J. T., & Sears, T. J. 2001, *Chem. Phys. Lett.*, 349, 547
- Zhu, R. S., Diau, E. G. W., Lin, M. C., & Mebel, A. M. 2001, *J. Phys. Chem. A*, 105, 11249